Tourinho, Paula S.; van Gestel, Cornelis A.M.; Morgan, A. John; Kille, Peter; Svendsen, Claus; Jurkschat, Kerstin; Mosselmans, J. Fred W.; Soares, Amadeu M.V.M.; Loureiro, Susana. 2016. **Toxicokinetics of Ag in the terrestrial isopod Porcellionides pruinosus exposed to Ag NPs and AgNO3 via soil and food**. *Ecotoxicology*, 25 (2). 267-278. 10.1007/s10646-015-1585-7

Contact CEH NORA team at
noraceh@ceh.ac.uk

Toxicokinetics of Ag in the terrestrial isopod *Porcellionides pruinosus* exposed to Ag NPs and AgNO$_3$ via soil and food

Paula S. Tourinho[1], Cornelis A.M. van Gestel[2], A. John Morgan[3], Peter Kille[3], Claus Svendsen[4], Kerstin Jurkschat[5], J. Fred W. Mosselmans[6], Amadeu M.V.M. Soares[1], Susana Loureiro[1]

[1]Department of Biology and the Centre for Environmental and Marine Studies, University of Aveiro, Aveiro, Portugal

[2]Department of Ecological Science, Faculty of Earth and Life Sciences, Vrije Universiteit Amsterdam, Amsterdam, The Netherlands

[3]Cardiff School of Biosciences, BIOSI 1, University of Cardiff, P.O. Box 915, Cardiff, CF10 3TL, UK

[4]Centre for Ecology and Hydrology, Maclean Building, Benson Lane, Crowmarsh Gifford, Wallingford, Oxfordshire OX10 8BB, UK

[5]Department of Materials, Oxford University, Begbroke Science Park, Sandy Lane, Yarnton, Oxford, OX5 1PF, UK

[6]Diamond Light Source Ltd., Harwell Science and Innovation Campus, Didcot, UK

Corresponding author:

Name: Paula S. Tourinho

E-mail: paulatourinho@ua.pt

Address: Departamento de Biologia & CESAM, Universidade de Aveiro,

Campus Universitário de Santiago, 3810-193 Aveiro, Portugal

Abstract

Silver nanoparticles (Ag NPs) have been used in numerous consumer products and may enter the soil through the land application of biosolids. However, little is known about the relationship between Ag NP exposure and their bioavailability for soil organisms. This study aims at comparing the uptake and elimination kinetics of Ag upon exposures to different Ag forms (NPs and ionic Ag (as $AgNO_3$)) in the isopod *Porcellionides pruinosus.* Isopods were exposed to contaminated Lufa 2.2 soil or alder leaves as food. Uptake and elimination rate constants for soil exposure did not significantly differ between Ag NPs and ionic Ag at 30 and 60 mg Ag/kg. For dietary exposure, the uptake rate constant was up to 5 times higher for Ag NPs than for $AgNO_3$, but this was related to feeding activity and exposure concentrations, while no difference in the elimination rate constants was found. When comparing both routes, dietary exposure resulted in lower Ag uptake rate constants but elimination rate constants did not differ. A fast Ag uptake was observed from both routes and most of the Ag taken up seemed not to be eliminated. Synchrotron X-ray fluorescence showed Ag in the S-cells of the hepatopancreas, thus supporting the observations from the kinetic experiment (i.e. low elimination). In addition, our results show that isopods have an extremely high Ag accumulation capacity, suggesting the presence of an efficient Ag storage compartment.

Keywords: Ag nanoparticles, bioaccumulation, exposure route, isopods, synchrotron

1. Introduction

Silver nanoparticles (Ag NPs) have been used extensively in industry over the last decades, especially due to their bactericidal properties (Durán et al., 2007). They are embedded in consumer products such as textiles, cosmetics, food packaging, and in materials and devices for medical purposes (Hendren et al., 2011).

The application of Ag NPs may result in the release of Ag from the consumer products, ending up in the aquatic environment, including the wastewater (Benn et al., 2010; Kim et al., 2010). In wastewater treatment plants, Ag nanoparticles may be present in effluents and sewage sludge (Kaegi et al., 2011). In many countries, the treated sewage sludge or biosolids is used as an agricultural amendment (Keller et al., 2013), and as a consequence Ag nanoparticles (and other Ag species) may reach the soil compartment. The land application of biosolids is considered the main route of Ag NPs to the terrestrial environment (Gottschalk et al., 2009).

To relate exposure of chemicals to bioavailability, uptake and elimination kinetic studies are useful. In a typical study, organisms are exposed to non-toxic concentrations during an uptake phase, followed by a depuration or elimination phase in clean medium. Body concentration of the chemical is measured in the test organisms at several points in time and a kinetic model is fit to the data. Uptake and elimination kinetic parameters, bioaccumulation factor (BAF) and half-life of chemicals can be obtained from these kinetic models. In this way, not only can kinetic studies provide valuable information for risk assessment (Nahmani et al., 2007), but it can also be very useful for regulatory purposes (Gobas and Morrison, 2000).

The bioaccumulation of Ag NPs and ionic Ag (from $AgNO_3$) has been evaluated in the earthworm *Eisenia fetida* after 28 days of exposure (Schlich et al., 2013; Shoults-Wilson et al., 2011). Schlich et al. (2013) showed slightly higher bioaccumulation factors (BAF) in earthworms exposed to Ag NPs, although the free Ag ion concentration in the soil was comparable for both Ag forms. Shoults-Wilson et al. (2011) found a lower BAF for Ag NP exposure, however, Ag bioaccumulation was not related only to Ag ions released from the nanoparticles. Up-to-date, only one study on the kinetics of Ag NPs in the springtail *Folsomia candida* is available in the literature (Waalewijn-Kool et al.,

2014). Ag NP bioaccumulation in the springtails was found to be lower than its ionic counterpart (as $AgNO_3$), but dissolved Ag concentration in the pore water could not explain total Ag uptake from Ag NPs (Waalewijn-Kool et al., 2014).

As the bioaccumulation process may differ between organisms (Ardestani et al., 2014), assessing Ag NP bioaccumulation in different organisms is essential to get a complete picture of their potential threats to the environment. For this purpose, isopods are suitable indicators of metal bioavailability (Dallinger et al., 1992; Hopkin et al., 1986; Loureiro et al., 2002; Udovic et al., 2009). They are known to accumulate high levels of metal in their hepatopancreas, which can accumulate up to 90% of total body metal burden (Hopkin and Martin, 1982). Kinetic studies with isopods are considered a better indicator of bioavailability than body burden measurements, since the flux of the contaminants into the organisms is more important in determining toxicity than total body concentration (van Straalen et al., 2005). Even though there are no standard protocols or guidelines to test bioaccumulation in isopods, the species *Porcellionides pruinosus* has been previously used successfully to evaluate the uptake kinetics of the pesticide lindane (Sousa et al., 2000; Loureiro et al. 2002). This species is able to dig into the soil and therefore stay in more direct contact with soil particles when compared to other isopod species that mainly live on the top soil (litter) layer Moreover, the isopod *Porcellionides pruinosus* can easily be collected and cultured under lab conditions.

The aim of the present study was to evaluate the uptake and elimination kinetics of Ag in the terrestrial isopod *Porcellionides pruinosus*, considering two forms of Ag: ionic (with $AgNO_3$) and nanoparticulate (Ag NPs). As different routes of exposure are essential to fully evaluate the bioavailability of contaminants in the environment (Ardestani et al., 2014; Loureiro et al., 2002; Sousa et al., 2000; Vijver et al., 2004; Vink et al., 1995), kinetic studies were conducted using soil and dietary exposures for comparison. In addition, and to understand and confirm results from uptake and elimination kinetics, µX-ray fluorescence mapping was carried out in isopods exposed to Ag NPs in soil.

2. Methodology

2.1. Test species and test chemicals

Specimens of the isopod *Porcellionides pruinosus* were collected in horse manure from an uncontaminated area in Coimbra (Portugal). The animals were kept in the laboratory at 20±2ºC and a 16/8h photoperiod for at least one month before the experiments. Adult males and non-gravid females (15-25 mg) in which no molting process could be observed were used.

Ag NPs and ionic Ag (as $AgNO_3$) were used to spike soil and food. Ag NPs (AMEPOX) were supplied dispersed in water at 1 g/L. They had a diameter size of 3-8 nm, with an alkane coating. Particle characterization was performed using Dynamic Light Scattering (DLS) in a Zetasizer nano ZS (Malvern instruments Ltd, Worcestershire, UK) and Zetasizer software 6.20 (Fig. S1). Also, Transmission Electron Microscopy (TEM) analyses were carried out on a JEOL JEM 2010 200 kV instrument (JEOL, Tokyo, Japan) (Fig. S2). For comparison to the ionic form, the soluble salt $AgNO_3$ (Sigma-Aldrich, 99% purity) was chosen.

2.2. Experimental setup – soil exposure

Lufa 2.2 soil (LUFA-Speyer 2.2, Sp 2121, LUFA Speyer, Speyer, Germany) was used in the kinetic tests and characterized as sandy loam with an organic carbon content of 2.3 ± 0.2%, pH_{CaCl2} of 5.6 ± 0.4, cation exchange capacity (CEC) of 10.0 meq/100 g and water-holding capacity (WHC) of 46.5%. Lufa 2.2 soil was spiked with Ag NPs or $AgNO_3$ as aqueous solution to reach two nominal concentrations of 30 and 60 mg Ag/kg dry soil. Concentrations were chosen based on results from a previous study (Tourinho et al., 2015) where the Ag NPs caused no toxicity at these concentrations. Therefore similar concentrations for Ag (as $AgNO_3$) were chosen for comparison. After adding the Ag solutions, the soil was manually mixed with a spoon. Additional water was added to moisten the soil to 45% of its maximum WHC. Spiked soil was left one day for equilibration before the exposures started. Soil pH_{CaCl2} was measured at the beginning of the experiment by shaking 5 g of soil with 25 ml 0.01 M $CaCl_2$ solution for 2 hours and measuring pH in the solution after settling of the soil particles.

The kinetic experiment consisted of two phases. During the uptake phase the animals were exposed to Ag-spiked soil for 21 days. Then, the animals were transferred to unspiked soil for a 21-day elimination phase. The animals were kept individually in plastic boxes ($\varnothing$ 65 mm), containing ~20 g of soil and fed alder leaves *ad libitum*. For each concentration, a total of 42 animals were used. The test was conducted in a climate room at 20º C and a 16 h light/8 h dark cycle. At time points of 1, 2, 4, 7, 10, 14, and 21 days of each phase, three isopods were sacrificed for Ag body concentration measurements. Isopods and soil were stored at -20ºC until Ag analysis.

2.3. Experimental setup – dietary exposure

Alder (*Alnus glutinosa*) leaves were cut into disks ($\varnothing$ 10 mm) and separated in groups by dry weight (d.w.). Two groups, containing ~40 leaf disks each, were soaked into 400 ml of Ag NPs dispersed in water at 10 or 20 mg Ag/L and shaken (150 rpm) for 4 days. The same procedure was conducted with $AgNO_3$ solutions to obtain ionic Ag dosed food. The leaves were left to dry at room temperature for one day before being offered as food. Isopods were placed individually in chambers containing a net and a plaster bottom (for details, see Loureiro et al. (2006)). For the uptake phase, Ag dosed alder leaves were offered *ad libitum* to the isopods for 21 days. After that, the Ag-dosed leaves were replaced by undosed leaves during the 21-day elimination phase. After 1, 2, 4, 7, 10, 14, and 21 days of uptake and elimination, food was removed from the chambers and the isopods were left in the chamber to empty their gut for one day. Then, animals were weighted and stored at -20ºC until total Ag analysis. The remaining food and faeces were dried at 45ºC for at least two days and their weight was recorded.

2.4. Total Ag analysis

Total Ag concentrations in isopods, soil and food were measured by Atomic Absorption Spectrometry (AAS). Soil (~130 mg) and leaf (~30 mg) samples were dried at 50ºC and then digested for 7 h in a mixture of concentrated HCl (J.T. Baker. purity 37%) and HNO_3 (J.T. Baker. purity 70%) (4:1. v/v) for 7 hours in closed Teflon containers, in an oven (CEM MDS 81-D) at 140ºC. After digestion, the samples were taken up in 10 mL of demineralized water

and analyzed for Ag by flame atomic absorption spectrometry (AAS; Perkin-Elmer AAnalyst 100). Soil samples, procedural blanks and reference material were analyzed in duplicates, while leaf samples were analyzed in one replicate due to the lack of material. Limit of detection (LOD) was 0.003 mg Ag/L, calculated as 3 times the standard deviation of the analytical standard blanks (n=20). Certified reference material (ISE sample 989 of River Clay from Wageningen, The Netherlands) was used to ensure the accuracy of the analytical procedure for soil samples. Recovery of Ag from the reference material was 100% (2.8 mg Ag/kg).

Isopods were freeze-dried, individually weighed and digested with a mixture of concentrated $HNO_3:HClO_4$ (7:1. v/v; J.T. Baker. ultrapure). The samples were evaporated to dryness and the residues were taken up in 1 mL 1M HCl. Ag content was determined by graphite furnace AAS (Perkin-Elmer 5100 PC). Procedural blanks were analyzed in triplicates. LOD was found to be 0.039 µg Ag/L (n=20).

2.5. µX-ray fluorescence mapping

Bio-imaging was undertaken at the Diamond Light Source (UK) I18 beamline (Mosselmans et al., 2009). Hepatopancreas samples were collected from isopods exposed to Ag NP-spiked food for 7 days. Food was spiked as described in the dietary experiment section, but using a solution concentration of 100 mg Ag/L. Freshly dissected hepatopancreas tubules were fixed overnight in 70% alcohol, embedded in low viscosity, hydrophilic, hard-grade LR White resin (Agar Scientific, Essex UK). The heat-polymerized blocks were sectioned at 0.5 µm with floatation on a diamond knife in an LKB Ultratome III. Sections were mounted on 50x25 mm fused quartz Vitreosil 077® slides (UQG Optics Ltd., Milton, Cambridge) in order to minimize the Si signal associated with conventional glass substrates, and were not stained in order to minimize interference with analytical signals. Slides were inserted into the standard I18 sample holder, and imaged 'externally' under brightfield conditions (Zeiss AxioVision optical microscope) for orientation purposes.

µX-ray fluorescence (XRF) data were collected using a Si(111) double crystal monochromator and the Kirkpatrick-Baez focusing mirrors, which provided a 3

7

µm spot size, were also used to remove harmonic contamination. The sample holder was positioned at 45° to the incident beam. The Ag K-edge at 25,531 eV is above the energy range of the I18 beamline and Ag L(III) edge Lα line (2,980 eV) is very close to the Argon Kα line (2,956 eV) hence the Ag L(II)-edge at 3,540 eV was used for mapping. However this provides a relatively insensitive signal as the Ag L edges have low fluorescence yield, with the Ag L(II) yield being lower than the Ag L(III) yield (Krause, 1979). Data were recorded using a 4-element Si drifts detector (Hitachi Inc.) positioned close to the specimen, whilst the Ar signal (from ambient air) was reduced but not eliminated by enclosing the specimen and detector inside a plastic bag under flowing He. Two XRF maps over the same region of the sample were collected using an incident energy below the Ag L(II) edge at 3,500 eV and one above the edge at 3,580 eV. The maps were then analyzed in PyMca 4.1.1 (Solé et al., 2007). The signal in the Ag Lβ energy window in the lower energy map was removed from the signal in the higher energy map, a procedure designed to remove the influence of the Ar Kβ peak at 3,190 eV from the Ag Lβ peak at 3,150 eV. Only the higher Ag regions are likely to be reflective of Ag, while the variations in the low levels are attributable to the noise in the subtraction method. This has been shown in our previous use of this methodology by recording Ag L(II) XANES spectra at high and low points (Diez-Ortiz et al., 2015). The S K-edge signal (2,308 eV) was measured at the same time. The samples were also mapped with an incident beam energy of 11,000 keV to produce element distribution maps for Cu (Kα = 8,046 eV).

2.6. Toxicokinetic models

Two kinetic models were tested to describe the uptake and elimination rates in isopods, named here as models 1 and 2. Model 1 is a classic first-order one-compartment model, in which the animals are considered as one unique compartment. Model 2 is also a first-order one-compartment model adapted from Vijver et al. (2006). In this model, an inert fraction is considered in the organism in which metals are stored and not eliminated during the elimination phase (Vijver et al., 2006).

In both models, uptake and elimination equations were fitted simultaneously. As metals naturally occur in the environment, the use of a background body concentration (C_0) is recommended (Skip et al., 2014). Therefore, C_0 was fixed by calculating the mean measured Ag body concentration at t=0.

For the uptake phase, the following equation was used in both models 1 and 2:

$$Q_{(t)} = C_0 + \frac{k1}{k2} \times C_{exp} \times (1 - e^{-k2 \times t})$$

(1)

where Q(t) = Ag internal concentration at t days (μg Ag/g_{animal}); C_0 = background internal concentration (μg Ag/g_{animal}); k1 = uptake rate constant ($g_{soil/food}$ / g_{animal} / day); k2 = elimination rate constant (day^{-1}); C_{exp} = Ag exposure concentration (mg $Ag/kg_{soil/food}$); and t = time (days).

For the elimination phase, two different equations were used in model 1 (Eq.2) and model 2 (Eq.3 – adapted from Vijver et al. (2006)), as follows:

$$Q_{(t)} = C_0 + \frac{k1}{k2} \times C_{exp} \times \left(e^{-k2 \times (t - t_c)} - e^{-k2 \times t}\right)$$

(2)

$$Q_{(t)} = C_0 + \frac{k1}{k2} \times C_{exp} \times \left[Fi + (1 - Fi) \times \left(e^{-k2 \times (t - t_c)}\right)\right]$$

(3)

where t_c = time the animals are transferred to clean medium (days) and F_i = inert fraction (ranging from 0 to 1).

For Ag NP exposure at 30 mg Ag/kg, it was necessary to constraint the parameter Fi to be <1.00, since Fi ranges from 0 to 1 (Vijver et al., 2006).

2.7. Statistical analysis

Uptake and elimination equations were fitted to the data and kinetics parameters were estimated using non-linear regression in SPSS (version 20). An F test was run to determine which of the two non-linear models with different number of parameters gave the best fit (Motulsky and Ransnas,

1987). Differences in k1 and k2 were tested by a Generalized Likelihood Ratio test and overlap of 95% confidence intervals, respectively. Half-life for elimination of Ag from the isopods after exposure to both test compounds was calculated as $\ln(2)/k2$, and Ag bioaccumulation factor (BAF) as $k1/k2$.

In the dietary exposure, feeding activity expressed as:

$Cr = (W_{Li} - W_{Lf})/W_{isop}$

$Ar = ((W_{Li} - W_{Lf}) - F)/W_{isop}$

$Ae = ((W_{Li} - W_{Lf}) - F)/(W_{Li} - W_{Lf}) * 100$

where Cr = consumption ratio (mg d.w. leaf/mg f.w. isopod); W_{Li} = initial leaf weight (mg d.w.); W_{Lf} = final leaf weight (mg d.w.); W_{isop} = initial isopod weight (mg f.w.); Ar = assimilation ratio (mg d.w. leaf/mg f.w. isopod); F = mass of faeces produced (mg d.w.); Ae = assimilation efficiency (%).

Feeding parameters were correlated to Ag body concentration in the isopods measured during the uptake phase using non-parametric Spearman correlation analysis in SPSS (version 20).

3. Results

3.1. Soil properties and Ag measurements

Soil pH_{CaCl2} in Ag spiked soils ranged from 5.47 to 5.50 (Table S1 – supporting information) and did not change in comparison to unspiked Lufa 2.2 soil (pH 5.49). Good recovery was obtained for Ag measurements in all soil samples, ranging from 81 to 124% (Table S1 – supporting information). Nominal concentrations of 30 and 60 mg Ag/kg resulted in measured concentrations of 37 and 48 mg Ag/kg for Ag NPs, and 27 and 70 mg Ag/kg for ionic Ag, respectively.

Ag concentration in alder leaves spiked with Ag NPs was found to be lower in comparison to leaves spiked with $AgNO_3$. For Ag NPs, concentrations were 534 and 832 mg Ag/kg$_{food}$, while for ionic Ag concentrations were 4499 and 4717 mg Ag/kg$_{food}$.

All toxicokinetic calculations in this paper are based on measured concentrations in soil and food.

The background of Ag concentration found in isopods (T0) was 2.30±1.32 µg Ag/g (mean±SD, n=3).

3.2. Uptake and elimination kinetics – soil exposure

No isopod mortality and weight change was observed during the 42-day experimental period (data not shown). After 21 days of uptake, mean Ag body concentration reached 90 and 136 µg Ag/g in isopods exposed to Ag NPs at 37 and 48 mg Ag/kg in soil, respectively. For ionic Ag, mean body concentration was 84 and 164 µg Ag/g at 27 and 70 mg Ag/kg, respectively. According to model 1, steady state body concentration was not reached in isopods exposed for 21 days to both Ag forms in soil during the uptake phase, although model 2 does suggest that steady state was reached (Fig. 1).

Ag kinetics parameters obtained by fitting model 1 (one-compartment model) and model 2 (one-compartment model with an inert fraction) are provided in Table 1. Best fit was obtained by model 2 for Ag NPs at 37 ($F_{1,39}=19.99$, $p<0.05$) and 48 mg Ag/kg ($F_{1,39}=20.37$, $p<0.05$), and for AgNO$_3$ at 27 ($F_{1,40}=6.99$, $p<0.05$) and 70 mg Ag/kg ($F_{1,38}=13.87$, $p<0.05$). For that reason, model 2 was chosen to describe the uptake and elimination kinetics of Ag in soil exposures. The fit of the models to Ag body concentration over time can be found in Fig. 1 (model 2) and Fig. S3 (model 1).

Values of k1 did not differ between the two exposure concentrations for Ag NPs ($X^2_{(1)}= 0.75$; n.s.) and ionic Ag ($X^2_{(1)}< 0.01$; n.s.). Moreover, no significant difference in k1 was found between both Ag forms at the two lower exposure concentrations (37 and 27 mg Ag/kg for Ag NPs and AgNO$_3$, respectively) ($X^2_{(1)}= 1.30$; n.s.) and the two higher concentrations (48 and 70 mg Ag/kg for Ag NPs and AgNO$_3$, respectively) ($X^2_{(1)}= 0.45$; n.s.).

No significant difference in k2 values was found between concentrations and Ag forms, based on overlap of the 95% of confidence intervals (Table 1).

Although it is suggested by model 1 that steady state Ag body concentrations were not reached, bioaccumulation factors (BAF) were calculated. BAF values were 3.0 for Ag NPs at both exposure concentrations, while BAF was 3.1 and 2.2 for ionic Ag at 27 and 70 mg Ag/kg, respectively.

3.3. Uptake and elimination kinetics – dietary exposure

Some mortality was observed in isopods during the food-exposure experiment, ranging from 11 to 16%. Possibly the moisture maintenance provided by the plaster bottom of the experimental chambers was not efficient enough and caused this mortality. Still, the fresh weight of surviving animals did not significantly change after the 42 days of experiment, indicating good health of the test animals (data not shown).

Mean Ag body concentration ranged from 370 to 414 μg Ag/g in isopods exposed to Ag NPs and from 435 to 658 μg Ag/g in isopods exposed to ionic Ag after 21 days of uptake. Model 2 failed to fit the data, so model 1 was used to describe Ag kinetics upon dietary exposure (Fig. 2).

Uptake and elimination rate constant (k1 and k2) for Ag NPs and $AgNO_3$ are shown in Table 2. It was observed that k1 did not significantly differ between the two exposure concentrations for Ag NPs ($X^2_{(1)}=2.74$; n.s.) and ionic Ag ($X^2_{(1)}=2.91$; n.s.). The 95% confidence intervals for the k2 values for the different treatments overlapped, suggesting no difference between treatments. However, k2 values were slightly lower for Ag NPs, resulting in higher BAF and half-life values compared to the ionic Ag exposures.

Food consumption ratio reached up to 0.21 and 0.28 mg food/mg isopod after 21-d of exposure to Ag NPs at 534 and 832 mg Ag/kg_{food}, respectively (Fig. S4). For $AgNO_3$, maximum food consumption ratio was 0.09 and 0.11 mg d.w. food/mg f.w. isopod after 21 days of exposure at 4499 and 4717 mg Ag/kg_{food}, respectively. Higher assimilation ratios were also observed in the Ag NP treatments, while assimilation efficiency was comparable between Ag NP and $AgNO_3$ treatments (Fig. S4). Egestion ratio was also found to be higher in isopods exposed to Ag NPs (data not shown) and was strongly influenced by consumption ratio (i.e., fecal production increased with increasing food consumption).

Ag NP and ionic Ag treatments showed similar patterns when relating feeding parameters with Ag body concentrations (Table 3; Fig. S4). A positive significant relationship was found between food consumption ratio and Ag body concentrations for all treatments (Spearman test, p<0.05). No significant relationship was found between assimilation ratio and Ag body concentrations (Spearman test, p>0.05), and a weak negative significant relationship was

found between assimilation efficiency and Ag body concentrations in all treatments (Spearman test, $p < 0.05$).

3.4. Synchrotron-based mapping of Ag in the hepatopancreas

Micro-focus X-ray fluorescence element mapping of anhydrously-prepared thin sections of the hepatopancreas of a woodlouse exposed to Ag-NP spiked leaves indicated that Ag was focally co-distributed with Cu and S specifically within the small 'S'-cells (Fig. 3). Mapping in the high-brightness synchrotron beam did not reveal Ag signals within the adjacent large 'B'-cells.

4. Discussion

In this study, the toxicokinetics of Ag NPs and ionic Ag (as $AgNO_3$) in the isopod *Porcellionides pruinosus* is described. This was combined with synchrotron μX-ray fluorescence (XRF) imaging technique to map the co-distribution of Ag and other elements in thin sections of the hepatopancreas of isopods exposed to Ag NPs.

4.1. Soil exposure

Upon soil exposure, Ag concentrations in the isopods increased with time for both Ag NPs and ionic Ag. This probably is due to the fact that the animals were hardly able to eliminate Ag, as little or no decrease in Ag body concentration was observed in the elimination phase (Fig. 1).

Uptake and elimination rate constants showed no significant differences between the two Ag forms. This could be a result of the route of exposure in hard-bodied organisms like isopods, which may be less exposed to the soluble fractions present in pore water (van Gestel and van Straalen, 1994). Uncoated Ag NPs and ionic Ag were found to have different time-dependent behavior in soils (Coutris et al., 2012). The Ag water-extractable and ion-exchangeable fractions were found to increase with time in soils spiked with Ag NPs, while they decreased in soils spiked with $AgNO_3$ (Coutris et al., 2012). Nevertheless, low porewater Ag concentrations (1.5% of total Ag in soil) were observed in Lufa 2.2 soil freshly spiked with Ag NPs and $AgNO_3$ (Waalenwijn-Kool et al. 2014). Since the authors have also used Lufa 2.2 soil

and the same Ag NPs, it is expected that low Ag porewater concentrations were present in soil samples.

Ag kinetics from both Ag NPs and AgNO$_3$ were best described by a one-compartment-model with an inert fraction (model 2). The inert fraction represents the metal storage fraction from which no metal elimination occurs during the elimination phase (Vijver et al., 2006). The high inert fraction (Fi) observed in the isopods confirms this hypothesis. Fi values were found to be 0.99 and 0.90 for Ag NPs and 0.87 and 0.82 for ionic Ag upon exposure to nominal concentrations of 30 and 60 mg Ag/kg dry soil, respectively. These values are well in agreement with other studies that have shown that up to 90% of total metal accumulated in isopods is detected in the hepatopancreas (Hopkin, 1990b). The isopod *Porcellio laevis* exposed to Cd-spiked food had >90% of the total Cd in the hepatopancreas (Odendaal and Reinecke, 1999; Odendaal and Reinecke, 2004). And when exposed to Zn-spiked food, the isopod *Porcellio scaber* had up to 70% (Donker et al., 1996) and 99% (Odendaal and Reinecke, 2004) of total Zn accumulated in the hepatopancreas. Van Straalen et al. (2005) showed that the amount of Zn in the hepatopancreas is dependent on exposure concentration, with between 40-60% and 80-90% of Zn in the hepatopancreas at exposure concentrations of 200 and 1,500 mg/kg dry food, respectively. Vijver et al. (2006) found relatively low Fi values of 0.43 and 0.55 for Cd and Zn in *Porcellio scaber* upon soil exposure, respectively.

The elimination rate constants for Ag found in this study were independent of the exposure route or of Ag exposure levels or Ag form. Interestingly, the Ag elimination rate constants were also in close agreement with the k2 values for Cd and Zn in the isopod *Porcellio scaber* reported by Vijver et al. (2006). The k2 values for *Porcellio scaber* were 0.19 and 0.18 day^{-1} for Cd and Zn exposures, respectively (Vijver et al., 2006), while k2 values for Ag in *Porcellionides pruinosus* varied from 0.15 to 0.26 day^{-1} for both the nanoparticulate and ionic Ag forms.

Waalewijn-Kool et al. (2014) performed a toxicokinetic study on Ag in the springtail *Folsomia candida*. Lower Ag elimination from AgNO$_3$ was observed in the springtails, resulting in higher BAF and half-life values in comparison to Ag NPs (Waalewijn-Kool et al., 2014). The same was not observed in our

study, where k2 values did not differ between Ag NPs and AgNO₃. It may suggest that isopods and springtails have different bioaccumulation kinetics for Ag NPs and AgNO₃. While isopods showed comparable accumulation and elimination capacity between Ag NPs and AgNO₃, springtails showed lower elimination for ionic Ag than for Ag NPs. In fact, in our study, a slightly higher inert fraction of Ag was found in isopods exposed to Ag NPs (0.90-0.99) when compared to isopods exposed to AgNO₃ (0.82-0.87). This might suggest a slightly different mechanism of accumulating both Ag forms.

4.2. Dietary exposure

Silver uptake and elimination kinetics for Ag NPs and AgNO₃ from contaminated food was described by a one-compartment model (model 1). Due to the spiking procedure (i.e. leaves soaked in Ag solution), final Ag concentrations were ~8.5 and 5.5 higher in food spiked with AgNO₃ than with Ag NPs, when soaked into solutions containing 10 and 20 mg Ag/L, respectively.

Higher uptake rate constants for Ag were found in isopods exposed to Ag NPs. However, these differences could be explained by the food consumption ratio. Isopods can avoid highly contaminated food by decreasing food consumption (Drobne and Hopkin, 1995; Loureiro et al., 2006; Zidar et al., 2012). Thus, the higher Ag concentration in AgNO₃-spiked food could be related to their lower food consumption (see Fig. S4).

The food assimilation ratio (mg assimilated food/ mg isopod) was not related with Ag body concentration. During food digestion, fluids and fine particles are separated from coarse particles in the primary and secondary filters in the proventriculus, going to the hepatopancreas afterwards. The coarse particles are voided and eliminated as fecal pellets after the digestive process (Hames and Hopkin, 1989). It is known that metals taken up with food may enter the body and reach the hepatopancreas without reaching other parts of the body (Vijver et al., 2006). This may explain the lack of a relationship between food assimilation and Ag assimilation (assessed as body concentration) in this study, considering that food and metals will show different assimilation pathways during the digestive processes.

Assimilation efficiency (percentage of assimilated food from ingested food) had a significant negative relationship with Ag body concentration for all treatments (Table 3). Higher assimilation efficiency indicates that the animal improved the nutritional gain from the ingested food. In this way, they avoided Ag uptake by consuming less contaminated food, and being less exposed to Ag.

No difference in the elimination rate constant was found between Ag NPs and AgNO$_3$. This is not surprising since k2 will be rather dependent on the organism (Crommentuijn et al., 1994; Díez-Ortiz et al., 2010), while k1 will depend on the exposure conditions, like the available metal concentration and the medium characteristics (Crommentuijn et al., 1994).

Usually, low elimination rate constants for metals in isopods exposed via food are found. Elimination rate constant for Cd was found to be zero in the isopods *Porcellio scaber* and *Oniscus asellus* (Crommentuijn et al., 1994), and low elimination capacity of Cd and Zn was observed in the isopod *Porcellio scaber* (Vijver et al., 2006). Also for Ag in the isopod *Porcellionides pruinosus* used in our study, elimination rates were low. This may result in a continuous increase of Ag accumulation in the isopods over time. The metal accumulation strategy in isopods is very efficient, nevertheless when storage limit is reached, it is very likely that toxicity will take place (Hopkin, 1990a; van Straalen et al., 2005).

4.3. Comparison between soil and dietary exposures

Oral uptake of contaminated soil and food is the main route of exposure in isopods (Koster et al., 2005; van Gestel and van Straalen, 1994; Vijver et al., 2006). Comparing the results obtained from model 1, uptake rate constants for Ag NPs and ionic Ag were lower upon dietary exposures than for soil exposures. Ag dietary uptake was controlled not only by exposure concentration, but also by the feeding activity (i.e., food consumption). It suggests that the avoidance of contaminated food, a typical behavior found in isopods, may have a great influence on Ag uptake. In soil, exposure concentration and ingestion of contaminated soil was probably the main factor affecting Ag uptake. However, it is not possible to determine whether the isopods were capable of avoiding the ingestion of contaminated soil or not.

Not much is known about the reason why isopods ingest soil particles, but it seems to be important for the digestive process in these organisms (Zimmer, 2002).

After ingestion of contaminated soil or food, the assimilation of pollutants in the body will be dependent on their bioavailability (i.e., desorption or dissolution from the medium inside the body). Organic matter content is an important factor that determines the bioavailability of metals when comparing soil and dietary exposures. Due to strong sorption of metals to organic matter, the high organic matter content in leaf material leads to greater sorption of metals when compared to soil (Sousa et al., 2000; Vink et al., 1995), especially of the loosely bound or free fractions of metal (Vijver et al., 2006). It may result in lower bioavailability of metals when exposed via food.

Elimination rate constants were found to be very low and comparable between both routes. It is suggested that elimination capacity in isopods is low and independent of the route of exposure. As uptake rate constants were higher upon soil exposure, higher BAF values for Ag were found in isopods exposed via soil.

Due to the low elimination capacity, Ag body concentrations remained almost constant during the elimination phase, and a significant part of the Ag seemed to be stored in an inert fraction. For soil exposures, it was possible to quantify this fraction using model 2, while for food exposures model 2 could not be fitted to the data. Nevertheless, it is clear from the data that elimination is slow also upon food exposure, and this may again be attributed to storage of the Ag. The storage of non-essential metals (with no elimination) is a main detoxification strategy in soil organisms, including isopods (Vijver et al., 2004). Our results suggest that Ag from both the Ag NPs and $AgNO_3$ was stored by the isopods rather than being eliminated. Interestingly, Ag storage and elimination from Ag NPs and ionic Ag were quite similar, suggesting that Ag NPs were also taken up as ionic Ag. In agreement with our finding, assimilation of dissolved Ag from ingested NPs was observed in the isopod *Porcellio scaber* exposed via food (Pipan-Tkalec et al., 2011).

4.4 Synchrotron µX-ray fluorescence mapping

Woodlice are acknowledged metal macro-accumulators (Udovic et al., 2009) with the midgut tubules, referred to as the hepatopancreas, serving as the main metal depository (Köhler et al., 1996). The tubules are comprised of two distinct types of epithelial cells: small pyramidal 'S'-cells containing Cu and sulphur-rich organelles, referred to as 'cuprosomes', with lysosome-like properties (Prosi and Dallinger, 1988); large binuclear 'B'-cells often containing copious lipid droplets and floccular Fe (and phosphate)-rich inclusions. 'S'-cells tend to accumulate soft Lewis acid metals with a high affinity for soft base S-donating ligands, whereas metals with hard acid properties tend to gravitate toward the hard base O-donating ligands within 'B'-cells (see Nieboer and Richardson, 1980, for definitions). Thus, it was unsurprising that micro-fluorescence mapping in a synchrotron beam located Ag, a weak Lewis acid like Cu, within the S-rich matrix of 'S'-cell cuprosomes of *Porcellionides pruinosus*. Similar observations were reported by Pipan-Tkalec et al. (2011) using a proton microprobe to map Ag in another terrestrial woodlouse species, *Porcellio scaber*, also fed a diet spiked with Ag NPs. Moreover, these authors deployed transmission electron microscopy to examine the hepatopancreas and corroborated our findings that aggregates of intact nanoparticles are absent within the epithelia. This indicates that the bound Ag within the cuprosomes derives from Ag^+ ion dissolution from nanoparticles. Whether the dissolution occurs within a region of the alimentary canal or within the presumably acidic matrix of the lysosome-like cuprosomes is at present unknown. Given the relatively long half-life of cuprosomes (Dallinger and Prosi, 1988), combined with the insolubility of metal-sulphur complexes (Allen et al., 1993), the Ag pool sequestered within isopod cuprosomes is unlikely to pose a significant toxicological challenge to the host organism or to its predators.

5.   Conclusions

High accumulation capacity of Ag from Ag NPs was observed in isopods exposed via soil and food. Our results suggest that Ag is accumulated in a storage compartment (i.e., hepatopancreas), as shown by the very low elimination rate constants. The elimination of Ag was independent of

exposure route and Ag form, showing that the storage strategy in isopods is a prevailing factor in Ag bioaccumulation. Due to slow elimination, Ag may be accumulated until it reaches toxic levels, and may pose a threat to terrestrial isopods in case of long-term exposure. Furthermore, because of the high levels accumulated in isopods, Ag might be transferred to possible predators. Biomagnification of Ag in the terrestrial environment therefore cannot be ruled out and should be further investigated.

Reference list

Allen HE, Fu G, Deng B (1993) Analysis of acid-volatile sulphide (AVS) and simultaneously extracted metals (SEM) for the estimation of potential toxicity in aquatic sediments. Environ Toxicol Chem 12:1441-1453

Ardestani MM, Van Straalen NM, Van Gestel CAM (2014) Uptake and elimination kinetics of metals in soil invertebrates: A review. Environ Pollut 193:277-295

Benn T, CaVanagh B, Hristovski K, Posner JD, Westerhoff P (2010) The release of nanosilver from consumer products used in the home. J Environ Qual 39:1875-1882

Coutris C, Hertel-Aas T, Lapied E, Joner EJ, Oughton DH (2012) Bioavailability of cobalt and silver nanoparticles to the earthworm *Eisenia fetida* Nanotoxicology 6:186-195

Crommentuijn T, Doodeman CJA, Doornekamp A, Van Der Pol JJ, Van Gestel CAM, Bedaux JJM (1994) Lethal body concentrations and accumulation patterns determine time- dependent toxicity of cadmium in soil arthropods. Environ Toxicol Chem 13:1781-1789

Dallinger R, Berger B, Birkel S (1992) Terrestrial isopods: useful biological indicators of urban metal pollution. Oecologia 89:32-41

Dallinger R, Prosi F (1988) Heavy metals in the terrestrial isopod *Porcellio scaber* Latreille. II. Subcellular fractionation of metal-accumulating lysosomes from hepatopancreas. Cell Biol Toxicol 4:97-109

Díez-Ortiz M, Giska I, Groot M, Borgman EM, Van Gestel CAM (2010) Influence of soil properties on molybdenum uptake and elimination kinetics in the earthworm *Eisenia andrei*. Chemosphere 80:1036-1043

Diez- Ortiz M, Lahive E, Kille P, Powell K, Morgan AJ, Jurkschat K, Van Gestel CAM, Mosselmans JFW, Svendsen C, Spurgeon DJ (2015) Uptake routes and toxicokinetics of silver nanoparticles and silver ions in the earthworm *Lumbricus rubellus*. Environ Toxicol Chem (in press). doi: 10.1002/etc.3036

Donker MH, Raedecker MH, Van Straalen NM (1996) The role of zinc regulation in the zinc tolerance mechanism of the terrestrial isopod *Porcellio scaber*. J Appl Ecol 33:955-964

Drobne D, Hopkin SP (1995) The toxicity of zinc to terrestrial isopods in a "standard" laboratory test. Ecotox Environ Safe 31:1-6

Durán N, Marcato PD, De Souza GI, Alves OL, Esposito E (2007) Antibacterial effect of silver nanoparticles produced by fungal process on textile fabrics and their effluent treatment. J Biomed Nanotechnol 3:203-208

Gobas F, Morrison HA (2000) Bioconcentration and biomagnification in the aquatic environment. Lewis Publishers: Boca Raton, FL.

Gottschalk F, Sonderer T, Scholz RW, Nowack B (2009) Modeled environmental concentrations of engineered nanomaterials (TiO2, ZnO, Ag, CNT, fullerenes) for different regions. Environ Sci Technol 43:9216-9222

Hames CAC, Hopkin SP (1989) The structure and function of the digestive system of terrestrial isopods. J Zool 217:599-627

Hendren CO, Mesnard X, Droge J, Wiesner, MR (2011) Estimating production data for five engineered nanomaterials as a basis for exposure assessment. Environ Sci Technol 45:2562-2569

Hopkin SP (1990a) Critical concentrations, pathways of detoxification and cellular ecotoxicology of metals in terrestrial arthropods. Funct Ecol 4:321-327

Hopkin SP (1990b) Species-specific differences in the net assimilation of zinc, cadmium, lead, copper and iron by the terrestrial isopods *Oniscus asellus* and *Porcellio scaber*. J Appl Ecology 27:460-474

Hopkin SP, Hardisty GN, Martin MH (1986) The woodlouse *Porcellio scaber* as a 'biological indicator' of zinc, cadmium, lead and copper pollution. Environ Pollut Series B, Chem Phys 11:271-290

Hopkin SP, Martin MH (1982) The distribution of zinc, cadmium, lead and copper within the woodlouse *Oniscus asellus* (Crustacea, Isopoda). Oecologia 54: 227-232

Kaegi R, Voegelin A, Sinnet B, Zuleeg S, Hagendorfer H, Burkhardt M, Siegrist H (2011) Behavior of metallic silver nanoparticles in a pilot wastewater treatment plant. Environ Sci Technol 45:3902-3908

Keller AA, McFerran S, Lazareva A, Suh S (2013) Global life cycle releases of engineered nanomaterials. J Nanoparticle Res 15:1-17

Kim B, Park C-S, Murayama M, Hochella Jr MF (2010) Discovery and characterization of silver sulfide nanoparticles in final sewage sludge products. Environ Sci Technol 44:7509-7514

Köhler H-R, Hüttenrauch K, Berkus M, Gräff S, Alberti G (1996) Cellular hepatopancreatic reactions of *Porcellio scaber* (Isopoda) as biomarkers for the evaluation of heavy metal toxicity in soils. Appl Soil Ecol 3:1-15

Koster M, Reijnders L, Van Oost NR, Peijnenburg WJGM (2005) Comparison of the method of diffusive gels in thin films with conventional extraction techniques for evaluating zinc accumulation in plants and isopods. Environ Pollut 133:103-116

Krause MO (1979) Atomic radiative and radiationless yields for K and L shells. J Phys Chem Ref Data 8:307-327

Loureiro S, Sampaio A, Brandão A, Nogueira AJA, Soares AMVM (2006) Feeding behaviour of the terrestrial isopod *Porcellionides pruinosus* Brandt, 1833 (Crustacea, Isopoda) in response to changes in food quality and contamination. Sci Total Environ 369:119-128

Loureiro S, Sousa JP, Nogueira AJA, Soares AMVM (2002) Assimilation efficiency and toxicokinetics of 14c-lindane in the terrestrial isopod *Porcellionides pruinosus*:

the role of isopods in degradation of persistent soil pollutants. Ecotoxicol 11:481-490

Mosselmans JFW, Quinn PD, Dent AJ, Cavill SA, Moreno SD, Peach A, Leicester PJ, Keylock SJ, Gregory SR, Atkinson KD and Rosell JR (2009) I18 - the microfocus spectroscopy beamline at the Diamond Light Source. J Synch Rad 16:818-24

Motulsky HJ, Ransnas LA (1987) Fitting curves to data using nonlinear regression: a practical and nonmathematical review. FASEB J 1:365-374

Nahmani J, Hodson ME, Black S (2007) A review of studies performed to assess metal uptake by earthworms. Environ Pollut 145:402-424

Nieboer E, Richardson DHS (1980) The replacement of the nondescript term 'heavy metals' by a biologically and chemically significant classification of metal ions. Environ Pollut (Series B) 1:3-26

Odendaal JP, Reinecke AJ (1999) The sublethal effects and accumulation of cadmium in the terrestrial isopod *Porcellio laevis* Latr.(Crustacea, Isopoda). Arch Environ Contam Toxicol 36:64-69

Odendaal JP, Reinecke AJ (2004) Evidence of metal interaction in the bioaccumulation of cadmium and zinc in *Porcellio laevis* (Isopoda) after exposure to individual and mixed metals. Water, Air Soil Poll 156:145-161

Pipan-Tkalec Ž, Drobne D, Vogel-Mikuš K, Pongrac P, Regvar M, Štrus J, Pelicon P, Vavpetič P, Grlj N, Remškar M (2011) Micro-PIXE study of Ag in digestive glands of a nano-Ag fed arthropod (*Porcellio scaber*, *Isopoda*, Crustacea). Nucl Instruments and Methods Phys Res Sect B 269:2286-2291

Prosi F, Dallinger R (1988) Heavy metals in the terrestrial isopod *Porcellio scaber* Latreille. I. Histochemical and ultrastructural characterization of metal-containing lysosomes Cell Biol Toxicol 4:81-96

Schlich K, Klawonn T, Terytze K, Hund- Rinke K (2013) Effects of silver nanoparticles and silver nitrate in the earthworm reproduction test. Environ Toxicol Chem 32:181-188

Shoults-Wilson WA, Reinsch BC, Tsyusko OV, Bertsch PM, Lowry GV, Unrine JM (2011) Effect of silver nanoparticle surface coating on bioaccumulation and reproductive toxicity in earthworms (*Eisenia fetida*). Nanotoxicology 5:432-444

Skip B, Bednarska AJ, Laskowski R (2014) Toxicokinetics of metals in terrestrial invertebrates: making things straight with the one-compartment principle. PloS one 9:e108740

Solé VA, Papillon E, Cotte M, Walter Ph, Susini J (2007) A multiplatform code for the analysis of energy-dispersive X-ray fluorescence spectra. Spectrochim Acta Part B 62**:**63-68

Sousa JP, Loureiro S, Pieper S, Frost M, Kratz W, Nogueira AJA, Soares AMVM (2000) Soil and plant diet exposure routes and toxicokinetics of lindane in a terrestrial isopod. Environ Toxicol Chem 19:2557-2563

Tourinho PS, van Gestel CAM, Jurkschat K, Soares AMVM, Loureiro S (2015) Effects of soil and dietary exposures to Ag nanoparticles and $AgNO_3$ in the terrestrial isopod *Porcellionides pruinosus*. Environ Pollut 205:170-177

Udovic M, Drobne D, Lestan D (2009) Bioaccumulation in *Porcellio scaber* (Crustacea, Isopoda) as a measure of the EDTA remediation efficiency of metal-polluted soil. Environ Pollut 157:2822-2829

Van Gestel CAM, Straalen NM (1994) Ecotoxicological test systems for terrestrial invertebrates. In: Donker MH, Eijsackers H, Heimbach F (eds) Ecotoxicology of soil organisms. CRC Lewis Publishers, Boca Raton, FL, Chelsea, MI, pp 205-228

Van Straalen NM, Donker MH, Vijver MG, Van Gestel CAM (2005) Bioavailability of contaminants estimated from uptake rates into soil invertebrates. Environ Pollut 136:409-417

Vijver MG, Van Gestel CAM, Lanno RP, Van Straalen NM, Peijnenburg WJGM (2004) Internal metal sequestration and its ecotoxicological releVance: a review. Environ Sci Technol 38:4705-4712

Vijver MG, Vink JP, Jager T, Van Straalen NM, Wolterbeek HT, Van Gestel CAM (2006) Kinetics of Zn and Cd accumulation in the isopod *Porcellio scaber* exposed to contaminated soil and/or food. Soil Biol Biochem 38:1554-1563

Vink K, Tompot A, Hermans M, Van Straalen NM, Dewi I, Bedaux J (1995) The importance of the exposure route when testing the toxicity of pesticides to saprotrophic isopods. Environ Toxicol Chem 14:1225-1232

Waalewijn-Kool PL, Klein K, Forniés RM, Van Gestel CAM (2014) Bioaccumulation and toxicity of silver nanoparticles and silver nitrate to the soil arthropod *Folsomia candida.* Ecotoxicol 23:1-9

Zidar P, Hribar M, Žižek S, Štrus J (2012) Behavioural response of terrestrial isopods (Crustacea: Isopoda) to pyrethrins in soil or food. Eur J Soil Biol 51:51-55

Zimmer M (2002) Nutrition in terrestrial isopods (Isopoda: Oniscidea): an evolutionary- ecological approach. Biol Rev 77:455-493

Table list

Table 1: Uptake and elimination kinetic parameters for Ag nanoparticles (NPs) and ionic Ag in isopods (*Porcellionides pruinosus*) exposed to Lufa 2.2 soil at nominal concentrations of 30 and 60 mg Ag/kg. 95% confidence intervals are given in between brackets

Table 2: Uptake and elimination kinetic parameters for Ag nanoparticles (NPs) and ionic Ag (as $AgNO_3$) in isopods (*Porcellionides pruinosus*) exposed to Ag-spiked alder leaves. Parameters were calculated using a one-compartment model (Equations 1 and 2). 95% confidence intervals are in brackets

Table 3: Spearman correlation coefficients (r^2) for the relation between feeding parameters (consumption ratio, assimilation ratio, assimilation efficiency) and Ag body concentrations in isopods (*Porcellionides pruinosus*) exposed to Ag NPs and ionic Ag contaminated food. Food concentration was 534 and 834 mg Ag/kg dry food for Ag NPs and 4499 and 4717 mg Ag/kg dry food for ionic Ag. Asterisks indicate significant correlation ($p < 0.05$)

Table 1: Uptake and elimination kinetic parameters for Ag nanoparticles (NPs) and ionic Ag in isopods (*Porcellionides pruinosus*) exposed to Lufa 2.2 soil at nominal concentrations of 30 and 60 mg Ag/kg. 95% confidence intervals are given in between brackets

Model	Ag form	Nominal concentration (mg/kg)	Measured concentration (mg/kg)	k1 (g_{soil}/g_{animal}/ day)	k2 (day^{-1})	Fi	BAF	half-life (days)
model 1	Ag NPs	30	37	0.19 (0.12-0.25)	0.01 (0.00–0.33)		16.2	59.6
		60	48	0.21 (0.15-0.27)	0.03 (0.00-0.04)		8.4	27.2
	Ionic Ag	30	27	0.21 (0.13-0.29)	0.02 (0.00-0.04)		9.7	31.7
		60	70	0.17 (0.11-0.22)	0.03 (0.00-0.05)		5.3	22.2
model 2	Ag NPs	30	37	0.79 (0.028-1.30)	0.26 (0.06-0.46)	0.99	3.0	
		60	48	0.57 (0.12-1.01)	0.19 (0.05-0.32)	0.91	3.0	
	Ionic Ag	30	27	0.46 (0.07-0.85)	0.15 (0.03-0.27)	0.87	3.1	
		60	70	0.48 (0.19-0.78)	0.22 (0.06-0.39)	0.82	2.2	

k1-uptake rate constant; k2-elimination rate constant; Fi-inert fraction; BAF-bioaccumulation factor; model 1- Equations 1 and 2; model 2 – Equations 1 and 3.

Table 2: Uptake and elimination kinetic parameters for Ag nanoparticles (NPs) and ionic Ag (as AgNO$_3$) in isopods (*Porcellionides pruinosus*) exposed to Ag-spiked alder leaves. Parameters were calculated using a one-compartment model (Equations 1 and 2). 95% confidence intervals are in brackets

	Concentration (mg Ag/kg$_{food}$)	k1 (g$_{food}$ / g$_{animal}$ / day)	k2 (day^{-1})	a	BAF	Half-life (days)
Ag NPs	534	0.028[a] (0.016 - 0.40)	0.004 (0.00– 0.025)	14.9	6.5	161
	832	0.019[a] (0.009 - 0.29)	0.011 (0.00 - 0.039)	15.8	1.7	61.9
Ionic Ag	4499	0.005[b] (0.004 - 0.007)	0.015 (0.001 - 0.028)	22.4	0.37	47.0
	4717	0.008[b] (0.00 - 0.012)	0.018 (0.00 - 0.044)	37.7	0.41	38.2

k1-uptake rate constant; k2-elimination rate constant; a – assimilation rate as Cexp * k1; BAF-bioaccumulation factor. Different letters [a,b] indicate significant differences between treatments.

Table 3: Spearman correlation coefficients (r^2) for the relation between feeding parameters (consumption ratio, assimilation ratio, assimilation efficiency) and Ag body concentrations in isopods (*Porcellionides pruinosus*) exposed to Ag NPs and ionic Ag contaminated food. Food concentration was 534 and 834 mg Ag/kg dry food for Ag NPs and 4499 and 4717 mg Ag/kg dry food for ionic Ag. Asterisks indicate significant correlation ($p<0.05$)

Ag form	mg Ag/kg	Feeding activity		
		Consumption ratio	Assimilation ratio	Assimilation efficiency
Ag NPs	534	0.83*	0.46	-0.66*
	832	0.79*	0.32	-0.60*
Ionic Ag	4499	0.84*	0.20	-0.67*
	4717	0.85*	0.16	-0.57*

Figure list

Fig. 1 Uptake and elimination kinetics of Ag from Ag NPs (circles) and ionic Ag as AgNO$_3$ (diamonds) in the isopod *Porcellionides pruinosus* exposed to nominal concentrations of 30 and 60 mg Ag/kg in Lufa 2.2 soil. Uptake and elimination phases lasted for 21 days each. Lines represent the modeled Ag body concentration, using model 2 (equations 1 and 3)

Fig. 2 Uptake and elimination kinetics of Ag NPs (circles) and ionic Ag as AgNO$_3$ (diamonds) in the isopod *Porcellionides pruinosus* exposed to Ag spiked alder leaves as food. Uptake and elimination phases lasted for 21 days each. Lines represent the modeled Ag body concentration, using model 1 (equations 1 and 2)

Fig. 3 µXRF maps of element distributions in an unstained LR White-embedded thin mid-tubule section of woodlouse (*Porcellionides pruinosus*) hepatopancreas exposed to dietary Ag NPs. (a) Light micrograph of a transverse section. Note that the morphology of the section is unclear due to a lack of differential contrast in the unstained sections. The outlines of some of the constituent 'S'-cells (S) and 'B'-cells (B) surrounding the lumen (Lu) are approximately delineated with dotted lines. Sulphur (b), Copper (c), and Silver (d) µXRF maps acquired across the entire section depicted in the micrograph. Note the relatively strong co-distributed Cu, S and Ag signals in 'S'-cells (arrow heads) but not in 'B'-cells
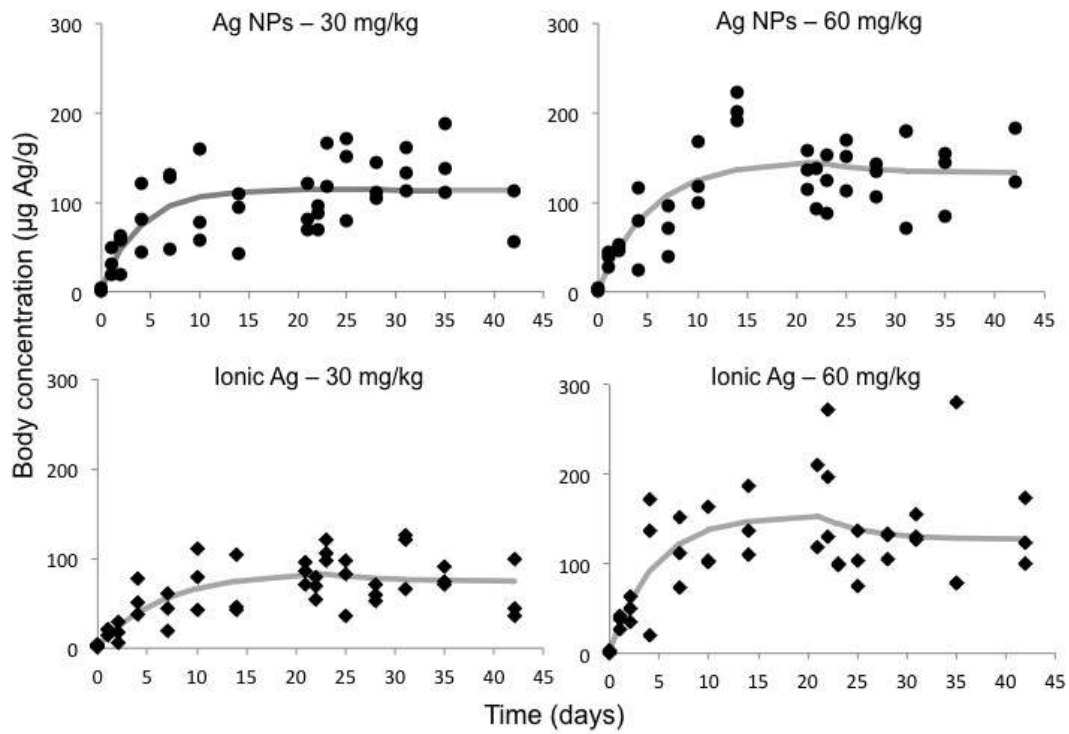
Fig. 1 Uptake and elimination kinetics of Ag from Ag NPs (circles) and ionic Ag as AgNO$_3$ (diamonds) in the isopod *Porcellionides pruinosus* exposed to nominal concentrations of 30 and 60 mg Ag/kg in Lufa 2.2 soil. Uptake and elimination phases lasted for 21 days each. Lines represent the modeled Ag body concentration, using model 2 (equations 1 and 3)
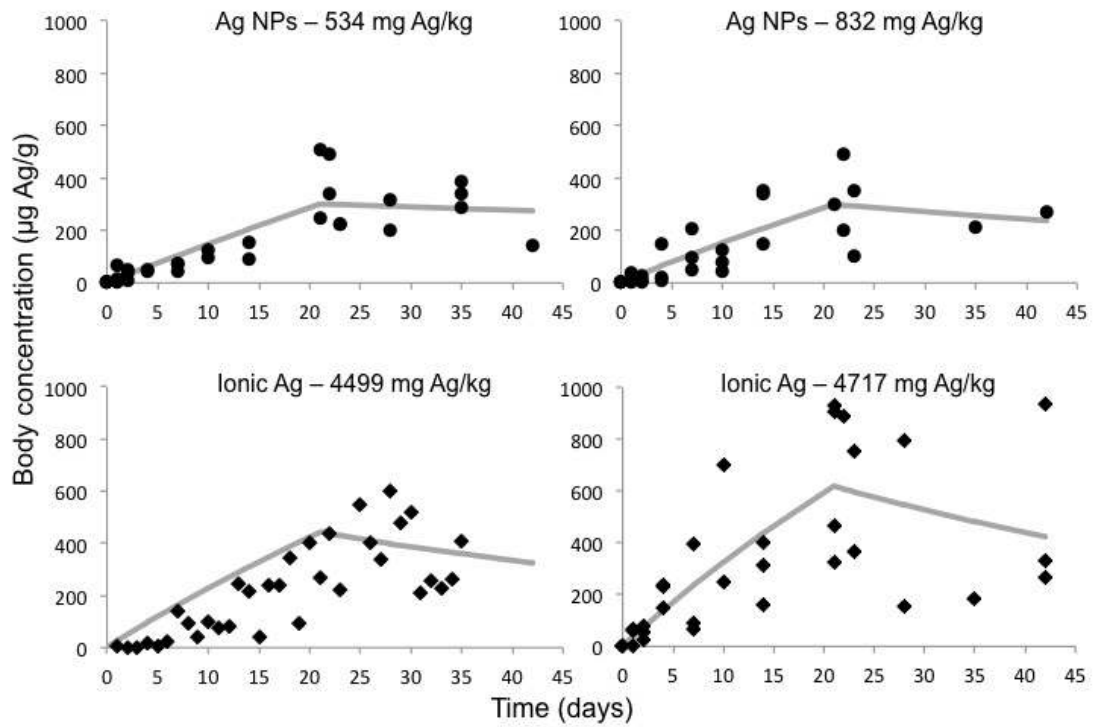
Fig. 2 Uptake and elimination kinetics of Ag NPs (circles) and ionic Ag as AgNO$_3$ (diamonds) in the isopod *Porcellionides pruinosus* exposed to Ag spiked alder leaves as food. Uptake and elimination phases lasted for 21 days each. Lines represent the modeled Ag body concentration, using model 1 (equations 1 and 2)
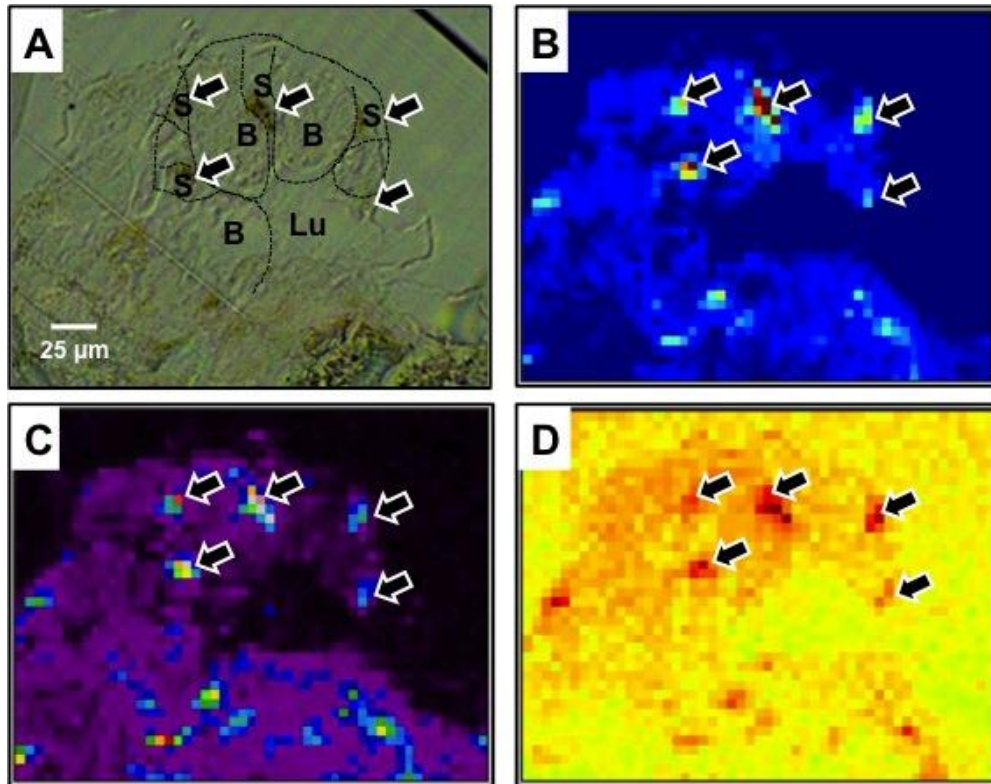
Fig. 3 µXRF maps of element distributions in an unstained LR White-embedded thin mid-tubule section of woodlouse (*Porcellionides pruinosus*) hepatopancreas exposed to dietary Ag NPs. (a) Light micrograph of a transverse section. Note that the morphology of the section is unclear due to a lack of differential contrast in the unstained sections. The outlines of some of the constituent 'S'-cells (S) and 'B'-cells (B) surrounding the lumen (Lu) are approximately delineated with dotted lines. Sulphur (b), Copper (c), and Silver (d) µXRF maps acquired across the entire section depicted in the micrograph. Note the relatively strong co-distributed Cu, S and Ag signals in 'S'-cells (arrow heads) but not in 'B'-cells